Simulations of the electrostatic potential in a thin silicon specimen containing a *p-n* junction

P.K. Somodi[1], R.E. Dunin-Borkowski[1], A.C. Twitchett[1], C.H.W. Barnes[2] and P.A. Midgley[1]
[1]Department of Materials Science and Metallurgy, University of Cambridge, Pembroke Street, Cambridge CB2 3QZ, U.K.
[2]Department of Physics, University of Cambridge, Madingley Road, Cambridge CB3 0HE, U.K.

ABSTRACT

The measurement of potentials associated with dopant atoms in semiconductors at nanometer spatial resolution using off-axis electron holography is known to be affected by the presence of the surfaces of thin specimens. In particular, the potential across a *p-n* junction is often found to be lower than would be expected from predicted properties of bulk devices. Here we present simulations of two-dimensional potential profiles within a thin (<1 μm) parallel-sided specimen containing a *p-n* junction. We find that the potential across the *p-n* junction is always smaller, when projected through the specimen, than would be expected from the properties of the bulk material. Crucially, the step in potential across the junction is independent of the value of the potential on the surface of the specimen for high dopant concentrations ($>10^{17}$ cm^{-3}). The simulations are compared with experimental data. Although they can account for some of the reduction in the observed potential, they do not fully explain the experimental results.

INTRODUCTION

The quantitative characterization of electrostatic potential distributions associated with the presence of dopant atoms is of fundamental importance for the development of future generations of nanoscale semiconductor structures and devices. Off-axis electron holography is a technique that offers the prospect of measuring electrostatic potentials at nanometer spatial resolution [1-3]. An electron wave that has passed through an electron-transparent specimen is interfered with another part of the same electron wave that has passed only through the vacuum. Analysis of the resulting interference fringe patterns allows the phase difference between the two parts of the electron wave to be established. This phase difference can then be related to the electrostatic potential within the specimen, V, by making use of the expression

$$\phi(x, y) = C_E \int V(x, y, z) dz \qquad (1)$$

where z is the electron beam direction, C_E is a constant that depends on the microscope accelerating voltage, and the geometry of the thin (< 1 μm) TEM specimen is defined in figure 1. Given an accurate measurement of the sample thickness it is possible to determine the potential within the specimen, averaged in the electron beam direction.

Previous electron holography studies have shown that the potential measured across a *p-n* junction, determined from measurements of the phase and specimen thickness according to equation 1, is almost always lower than would be predicted using simple theory [4, 5]. There are several possible explanations for this discrepancy including the effects of surface depletion, the implantation of ions during sample preparation and electron-beam-induced charging of oxide

layers on the specimen surface. By calculating the potential within a thin specimen we aim to show how the surfaces of a finite specimen can partially account for the discrepancies observed.

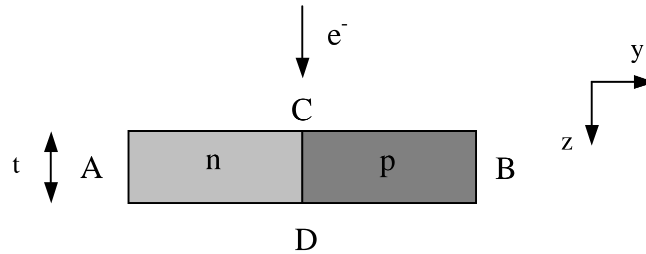

Figure 1. Schematic diagram showing the direction of the electron beam relative to a parallel-sided TEM specimen of thickness *t* containing a *p-n* junction. A and B represent the boundaries of the simulation, at which the semiconductor is defined to behave as either pure *n*-type (A) or *p*-type (B) material. C and D represent the surfaces that are taken to be equipotentials.

SIMULATION DETAILS

As the devices described below do not exhibit significant quantum confinement, due to the nature of their design, simulations were carried out by solving standard semi-classical semiconductor equations in a thin TEM specimen [6]. As the equations are non-linear, finite element methods are used to solve them, using an algorithm that is based on code described in reference 7. Far from the junction the specimen is assumed to behave as if it were an isolated semiconductor of either *n*- or *p*- type material. The boundary conditions on the surfaces that are labelled A and B in figure 1 reflect this condition. A key experimental observation is that TEM specimens almost never show electrostatic fringing fields outside their surfaces close to the positions of *p-n* junctions [8]. The specimen surfaces (labelled C and D in figure 1) are therefore treated as equipotentials in the present study. Previous work on simulations of *p-n* junctions in TEM specimens [9] has instead assumed the presence of charged oxide layers on the surface. For a clean (1 1 1) surface of silicon, the surface energy is 0.7 eV below the conduction band energy [10]. However the true value of the potential on the surface of a TEM specimen is unknown and will be affected by sample preparation.

SIMULATION RESULTS

Representative results of simulations for a parallel-sided specimen containing an abrupt, symmetrical silicon *p-n* junction are shown in figure 2, for dopant concentrations of 10^{19}, 10^{18}, 10^{17} and 10^{16} cm^{-3}. The dopant atoms are Sb (*n*-type) and B (*p*-type), and the surface state energy is set to 0.7 eV above the Fermi level. Equipotential contours of spacing 0.05eV are shown in each figure. The thickness of each specimen in the electron beam direction is 300 nm. This is a representative thickness for a sample examined using electron holography, as it is thin enough to minimize inelastic scattering but thick enough for contrast to be visible. Qualitatively figure 2 shows that setting the surface to be an equipotential affects the potential within the specimen well below its surface, particularly for low dopant concentrations.

Experimentally, only the potential projected in the electron beam direction (the *z*-direction in figure 1) is measured using electron holography. Simulated projected potential profiles, which have been calculated from the results shown in figure 2 are shown in figure 3. For comparison,

the potential profiles predicted on the basis of the bulk properties of the device are also shown. There is a clear reduction in the potential measured across the junction for the samples of finite thickness compared to the bulk profile. This reduction in the potential step across the junction is shown as a function of sample thickness in figure 4. Significantly, it is found that the step in potential is always lower than the value expected in the bulk. In particular, for samples of small thicknesses the dopant contrast across the junction will be unobservable using electron holography. Figure 5 shows the apparent depletion widths that would be inferred from the projected potential profiles. For lower dopant concentrations and small sample thicknesses, the variation in projected potential across the junction is so small that it becomes impossible to calculate the depletion width accurately.

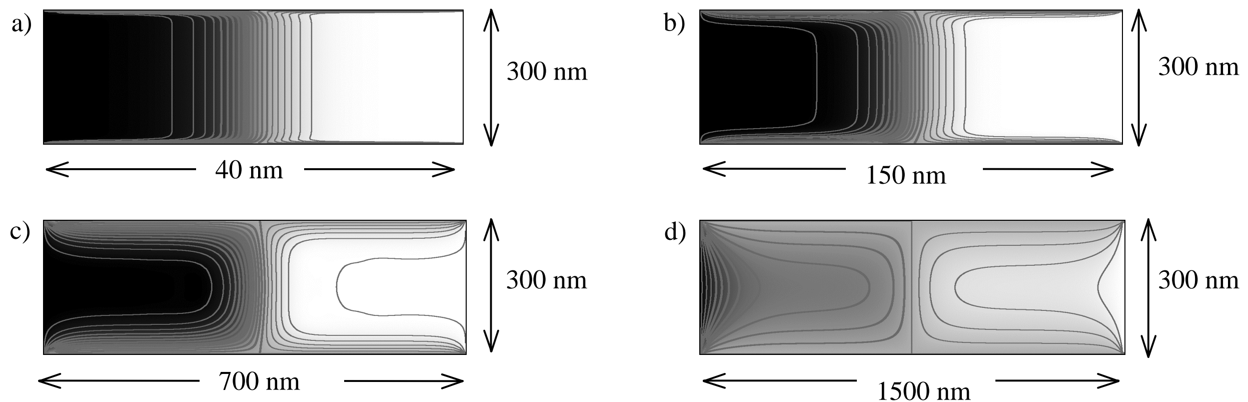

Figure 2. Simulations of electrostatic potential distributions in parallel-sided slabs of thickness 300 nm containing abrupt, symmetrical Si *p-n* junctions formed from a) 10^{19} , b) 10^{18} , c)10^{17} and d) 10^{16} cm^{-3} of Sb (*n*-type) and B (*p*-type) dopants. The potential at the surfaces of each specimen is taken to be 0.7 eV above the Fermi level. Contours of spacing 0.05 V are shown. The horizontal scale is different in each figure in order to show the variation in potential close to the position of the junction.

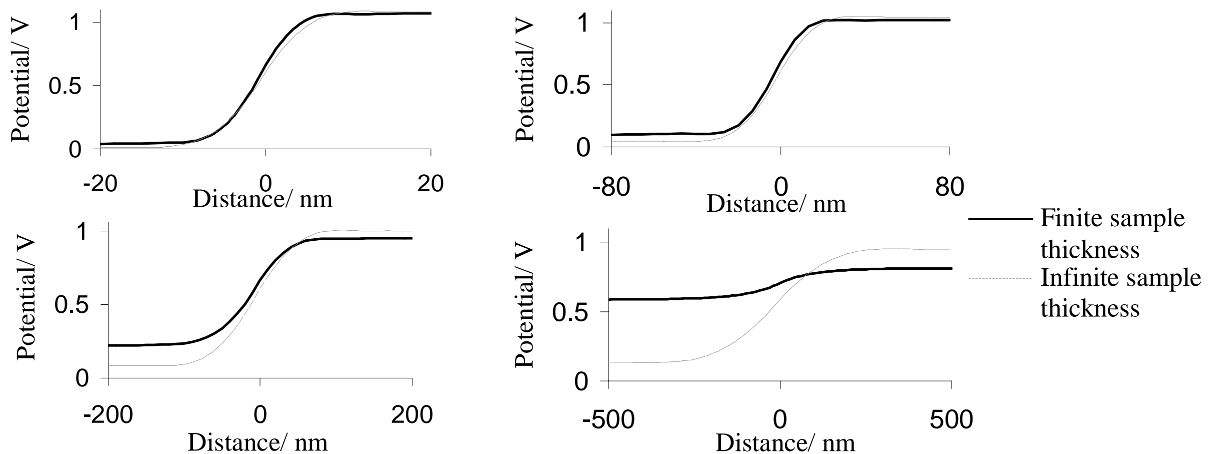

Figure 3. The projected conduction band energy relative to the Fermi level, averaged through the thickness of the specimen in a direction perpendicular to its surface, determined from the simulations shown in figure 2. The dopant concentrations are a) 10^{19} , b) 10^{18} , c) 10^{17} and d) 10^{16} cm^{-3}. The dashed lines represent the conduction band energies for bulk-like material.

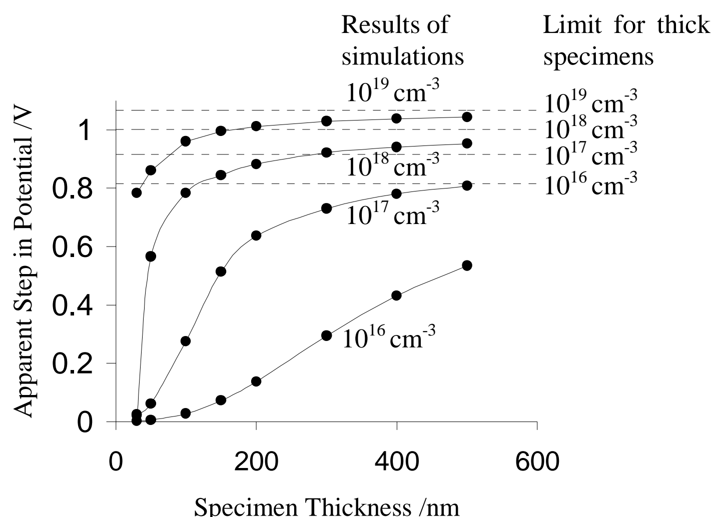

Figure 4. The step in potential across the junction plotted as a function of specimen thickness for the dopant concentrations indicated. The dashed lines represent the value expected for an infinite specimen thickness. The potential on the surface is taken to be 0.7eV below the conduction band.

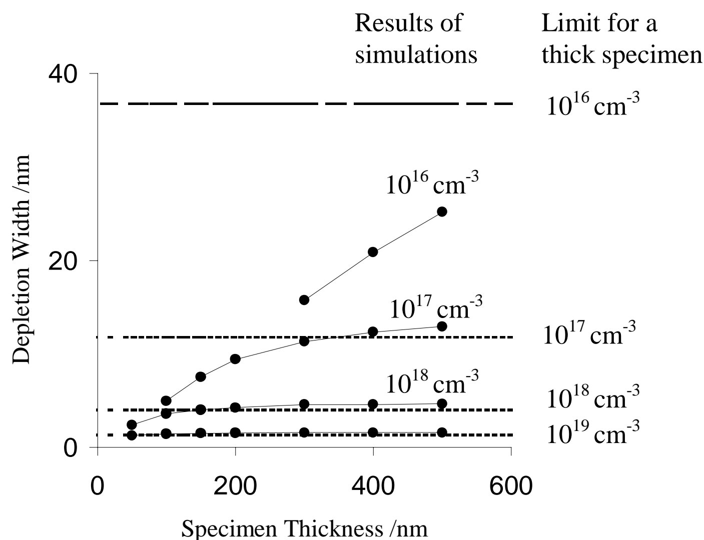

Figure 5. The depletion width that would be inferred from the *projected* potential profiles, plotted as a function of specimen thickness. The dashed lines represent the potential that would be expected for a sample of infinite thickness. The potential on the surface is taken to be 0.7eV below the conduction band. Crucially, the potential difference across the junction is approximately independent of the value of the potential taken at the surface of the specimen when the dopant concentration is high ($>10^{17}$ cm^{-3}), as shown in figure 6.

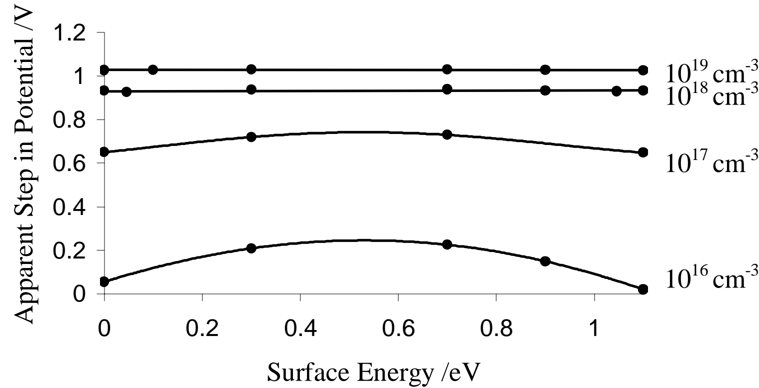

Figure 6. The variation in the apparent step in potential across the *p-n* junction, plotted as a function of the surface energy (measured relative to the Fermi level).

COMPARISON WITH EXPERIMENTAL RESULTS

Figure 7 shows a potential profile across a focussed ion beam milled silicon *p-n* junction measured using off-axis electron holography [8]. The dopant atoms are Sb (*n*-type) and B (*p*-type). The dopant concentrations were determined, using secondary ion mass spectrometry (SIMS), to be 3 x 10^{-18} cm^{-3} in the *n*-type region and 4 x 10^{-18} cm^{-3} in the *p*-type region. The sample thickness, determined using convergent beam electron diffraction, was 390 nm. The experimental profile is compared with a simulated profile for the same dopant concentrations and sample thickness in figure 7. The depletion width is found to be larger and the step in potential across the junction found to be smaller in the experimental results. Based on this comparison we speculate that sample preparation may have resulted in a reduction in the electrically active dopant concentration within the specimen and that additional damaged or implanted layers may be present on the specimen surfaces, as well as the effect of the presence of the specimen surfaces on the potential within the specimen.

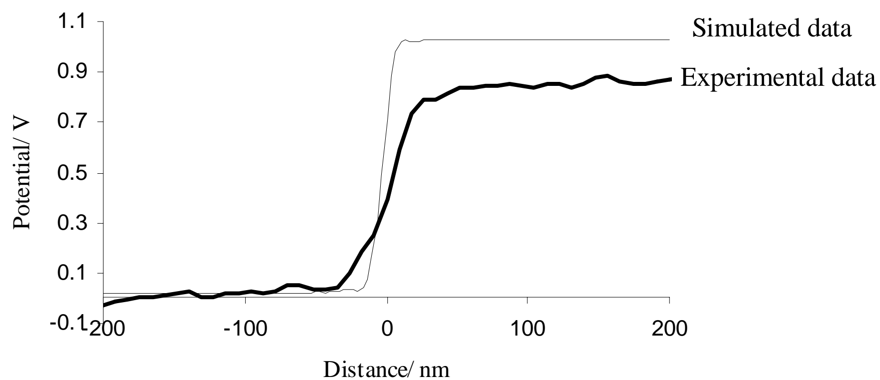

Figure 7. The potential profile across a *p-n* junction measured from a focussed ion beam milled specimen of crystalline thickness 390 nm using off-axis electron holography. The dopant atoms are Sb (*n*-type) and B (*p*-type) with nominal concentrations of 3 x 10^{-18} cm^{-3} and 4 x 10^{-18} cm^{-3}, respectively. The simulation was performed for these parameters and for a surface state energy of 0.7 eV.

CONCLUSIONS

The projected potential step across a *p-n* junction located within a thin specimen is always reduced from predictions, based on the properties of bulk devices, due to the presence of the specimen surfaces. For low dopant concentrations the step in potential is reduced significantly. However, the potential across the junction is found to be independent of the value of the potential on surface of the specimen for high dopant concentrations. Providing that the surface is an equipotential, the exact nature of the surface may not be important. In the literature, the reduction in the observed potential is often explained by introducing a crystalline layer of electrically inactive material on the surface of the specimen, known as a 'dead layer' [11,12]. Given the results presented here, we believe this term is misleading, and that experimentally the reduction in the potential can result, in part, simply from surface depletion.

Further work will involve the study of the effects of sample damage and implantation during sample preparation to account for remaining discrepancies between the simulations and experimental measurements. The need for a reliable 3-d nano-scale resolution profiling technique [13] also highlights the need for 3-d simulations of the potential in slab-shaped and wedge-shaped specimen geometries.

ACKNOWLEDGMENTS

We are grateful to the EPSRC, the Royal Society and Newnham College, Cambridge for financial support. We also thank Tim Yates for his help in producing figure 2.

REFERENCES

[1] R.E. Dunin-Borkowski, M.R. McCartney and D.J. Smith, in Volume 3 of the *Encyclopaedia of Nanoscience and Nanotechnology*, edited by H.S. Nalwa (American Scientific Publishers, 2004), pp. 41-100.

[2] *Introduction to Electron Holography,* edited by E. Völkl, L.F. Allard, and D.C. Joy, (Kluwer Academic/ Plenum Publishers, New York, 1998).

[3] L. Reimer, *Transmission Electron Microscopy*, (Springer–Verlag, Berlin, 1991).

[4] A.C. Twitchett, R.E Dunin-Borkowski, and P.A Midgley, Phys. Rev. Lett. **88**, 238302 (2002).

[5] W.D. Rau P. Schwander, F.H. Baumann, W. Hoppner, and A. Ourmazd, Phys. Rev. Lett. **82**, 2614 (1999).

[6] S.M. Sze, *Semiconductor Device,* (Wiley, Singapore, 2002) 2nd ed. Chapt. 4.

[7] H.P. Langtangen, *Computational Partial Difference Equations*, (Springer, 2003), Chapt. 2.

[8] A.C. Twitchett, R.E Dunin-Borkowski, R.J. Halifax and P.A Midgley, J. Phys.: Condens Mat., **16**, S181-S192, (2004).

[9] M. Beleggia, P.F. Fazzini, P.G. Merli and G. Pozzi, Phys. Rev. B, **67**, 045328 (2003).

[10] H. Lüth, *Solid Surfaces, Interfaces and Thin Films*, (Springer, Heidelberg, 2001) 4th ed., p. 349.

[11] A.C. Twitchett, R.E. Dunin-Borkowski, R.J. Halifax, R.F. Broom and P.A. Midgley, J. Microsc. **214**, 287-296, (2004).

[12] Z. Wang, T Hirayama, K Sasaki, H Saka and N Kato, Appl. Phys. Lett. **80**, 246 (2002).

[13] International Technology Roadmap for Semiconductors (Semiconductor Industry Association, San Jose, CA, 2003), 2003 Edition; http://public.itrs.net/.